Optimum Biasing for Cell Load Balancing Under QoS and Interference Management in HetNets

EDENALISOA RAKOTOMANANA, (Student Member, IEEE),
AND FRANÇOIS GAGNON, (Senior Member, IEEE)

Lacime laboratory, Department of Electrical Engineering, École de technologie supérieure, Montréal, QC H3C 1K3, Canada

Corresponding author: E. Rakotomanana (edenalisoa.rakotomanan@lacime.etsmtl.ca)

ABSTRACT In this paper, we consider a network in which lower power nodes (LPNs) are deployed jointly within macrocells. However, there are significant differences between the transmit power levels, coverage areas, and deployment densities of these two types of base stations. Such disparities lead to an unfair load distribution, as well as a lower throughput for picocells' users equipments (UEs). A good solution to such issues is the exploitation of the cell range expansion (CRE) technique. Although CRE has widely proven its effectiveness, it may degrade the network capacity if the cell bias is not chosen properly. In fact, it may generate severe intercell interference at extended region cell (ERC) UEs, which leads a deterioration of their throughput. We thus propose a downlink coordinated cell range expansion for mobility management (CCREMM) strategy that analytically computes the joint optimal bias at picocells and macrocells. CCREMM mitigates the interference at ERC-UEs by accounting for their maximum tolerable interference. Moreover, CCREMM reaches the load balancing and the UE QoS satisfaction by accounting for additional parameters. It will be proven that our strategy which is associated with the maximum throughput scheduling technique, results in a cell load-balancing improvement, fairness, and a 50–90% UE throughput enhancement. These performance figures are shown to surpass those achieved by alternative approaches proposed in the existing literature.

INDEX TERMS HetNets, load balancing, resource allocation, QoS, mobility management.

I. INTRODUCTION

Small cell network has attracted much attention due to the explosive demand of UEs data requirement. In order to satisfy these requirements, future wireless can be envisioned to have operator deployed macrocells providing a coverage blanket, along with picocells, low-powered user-deployed femtocells, and user/operator-deployed low-powered wifi access points (APs) [1], [2]. The resulting networks are generally referred to as heterogeneous networks (HetNets). LPNs together with macrocells, can improve the coverage and capacity of cell-edge users and hotspot by exploiting the spatial reuse of spectrum [3]. In an heterogeneous cellular network, each tier differs in transmission power, path loss exponent, deployment density and bandwidth [4], [5]. As mentioned in the literature, pico BSs (PBS) transmission power is 250–mW 2 W while that of macro BS (MBS) is 5 W–40 W [1] which leads to a large power disparity of about 20 dB. However, apart from the benefit obtained through the deployment of cells heterogeneity, the power

variability between BSs involves the so-called load imbalance in practically all types of networks. This behaviour could be explained by the fact that most UEs tend to connect to the most powerful MBS, from which they receive the maximum signal strength [6] although it is located closer to a PBS than a MBS. Thus, we deduce that various challenges are implied by the deployment of HetNets. Among them, the capacity, coverage, mobility management (MM), user association (UA) and load balancing (LB) across multiple network tiers [7] are usually cited. Particularly, MM, UA and LB are the most important key elements in HetNets to ensure a continuous connectivity to UEs while maintaining satisfactory quality of service (QoS) [8].

To overcome the load imbalance problem in HetNets, using a LB technique is crucial. Load balancing is aimed at optimizing resource usage while achieving efficient resource utilization, efficient BSs utilization, and equal BSs load. Additionally, it enables throughput maximization and response time minimization, and it avoids overload of any

single resource. One efficient suboptimum technique of LB is the CRE standardized by the 3rd Generation Partnership Project (3GPP) in the last decade. According to this concept, each serving and neighboring small cell virtually expands their coverage area by adding a virtual offset to their DL received signal strength (RSS) pilot signal at UEs. As demonstrated in several works, CRE permits an efficient load balancing in HetNets. Nevertheless, it may result in severe ICI at the ERC-UEs which may deteriorate the throughput of these UEs. The resulted interference can be explained by the fact that UEs associated with the ERC are not served by the BS that provide them the strongest RSS.

Consequently, in this paper, we will exploit the efficiency of the aforementioned CRE to design our CCREMM strategy. CCREMM is based on a combined objective function (COF) formed by several parameters. Then, via the COF, the optimal value of each BS offset is computed and a maximum performance in terms of throughput, signal-to- interference-noise ratio (SINR), fairness and network load balancing is obtained.

The following is a review of the existing work regarding the optimization of the UA and MM based on CRE for cellular networks. Firstly, authors in [9] propose a coordinated cell range expansion (CCRE) technique, in which the optimal biases for macrocell and picocell are found by using the concept of reinforcement learning technique and intercell coordination. Through simulations, it is shown that, with their strategy, the handover and UE throughput performance in HetNets is enhanced compared to the classical CRE-MM technique. However, UE QoS requirements and maximum tolerable interference at ERC-UEs are not taken into account, and a multi-arm bandit (MAB) approach is utilized. In [10], authors focus on the classical range expansion of picocells and they propose jointly an intercell interference coordination (ICIC) technique to enhance picocell performance. Picocell bias is computed analytically through a geometrical approach and interference problem is solved by a linear programming optimization. In contrast to [10], we attempt to expand the range of both macrocell and picocell. Moreover, interference at ERC-UEs is mitigated by using an interference limitation factor imbricated in a special COF. In [11], a joint heuristic CRE and ICIC is proposed in which CRE is achieved by offloading UE to the BS for which it has the minimum pathloss. The ICI problem in ERC is then solved by applying a resource partitioning scheme where MBS lowers their power on a fraction of the spectral or temporal resources which can then be used by ERC-UEs. Resource partitioning is also used in [12] to mitigate ICI at ERC-UEs. In [13], the authors propose a SINR and a rate-based CRE methods. They analytically compute the homogeneous bias values to be assigned to each small cell. In fact, SINR and rate are multiplied by a biasing factor to find the final bias values of picocells. Illustrated through simulations, the method results in a fairer distribution of traffic. In [14], the authors investigate DL performance under pico-CRE with various bias settings reinforced by an ICIC technique. Hence, identical power offsets are assumed for all picocells in HetNets.

Actually in [14], ICIC is implemented using the lightly loaded CCH transmission subframe (LLCS) in long term evolution (LTE)-Advanced. Through simulations, improved performance is observed in terms of interference mitigation. In [15], a reinforcement learning technique is used to determine the appropriate bias value for CRE and authors focus on the minimization of the UE outage number rather than the ICI.

In this paper, we make specifically the following contributions:
- We formulate a COF containing an interference limitation factor for ECR-UEs, a UE QoS satisfaction factor, and a cell load factor;
- Then, we formulate new macrocell and picocell utility functions from the COF to design our CCREMM for HetNets;
- Thereafter, we derive analytical expressions for optimal heterogeneous range expansion offset (REO) for macrocells and picocells;
- Finally, a highly efficient scheduling strategy called MTS is used jointly with our proposed CCREMM, and the gain from this combination is shown through computer simulations.

The rest of the paper is organized as follows. In Section 2, the system model used in the work is described, and some general definitions are given. In Section 3, the proposed coordinated cell range expansion for mobility management strategy is developed. In Section 4, simulation results are presented to demonstrate how the CCREMM significantly improves UE and network throughput, UE SINR, and UE fairness. Finally, Section 5 concludes this paper.

II. SYSTEM MODEL

In this paper, we consider a DL two-layer LTE HetNets, which is comprised of a set of macrocells, each having the same number of indoor picocells deployed and overlaid within their coverage area. Picocells, also known as lower power nodes, have a lower transmission power and provide narrower coverage than macrocells.

We denote by $I = M \cup P$, the set of BSs in HetNets with a set $M = \{1, \ldots, M\}$ of macrocells underlaid by a set $P = \{1, \ldots, P\}$ of picocells. MBSs form a regular three-sector hexagonal cellular network denoted by $m \in M$ and PBSs. denoted by $p \in P$ are randomly distributed within each MBS's sectors. The set of UEs is represented as $U = \{1, \ldots, U\}$, where UEs associated to macrocells are referred as macrocell UEs (MUEs), denoted as $U_m(i) = \{1_m(i), \ldots, U_m(i)\} \in U$, $1 \le i \le M$ and UEs served by picocells are referred as picocell UEs (PUEs), denoted as $U_p(i) = \{1_p(i), \ldots, U_p(i)\} \in U$, $1 \le i \le P$, where $U_m \ne U_p$. Users are randomly dropped within a circle around each picocell p. Each UE $k(i)$ with $k \in U_p$ or U_m and $i \in \{m, p\}$ has a fixed velocity $v_{k(i)} \in V km/h$ and a random direction of movement within an angle of $[0, 2\pi]$. Picocells and macrocells operate with a bandwidth B consisting of $r = \{1, \ldots, R\}$ resource blocks (RBs) which are basic unit elements of a standard [24].

At each transmission time interval (TTI) of duration $1ms$, each BS $i \in \{m, p\}$ decides to expand its coverage's range through a power offset, called REO resulting from analytical expressions produced by new macrocell and picocell utility functions. The macrocell and picocell utility functions result from a so-called COF containing three major parameters related to user QoS requirements, cell load and interference boundary. Subsequently, REO is incorporated into a BS-UE association or/and into a handover decision policies in order to enhance the cell load balancing, the user throughput and fairness. The three major parameters of the COF are described below.

The first parameter represents the average QoS factor in terms of a target SINR of all UEs associated with a given BSi, it is defined as Γ_k. In this work, we assume that a heterogeneous wireless environment has different types of users with differentiated QoS targets. In particular, these QoS requirements can be written as:

$$y_{i,k,r} \geq \Gamma_k \tag{1}$$

in which, $y_{i,k,r}$ is the DL-SINR of user k, $\forall k \in U$ served by BS i, $\forall i \in I$ in resource block (RB) r and Γ_k is the UE target SINR. The UE DL-SINR is modeled in [16] as:

$$y_{i,k,r} = \frac{L_{M,k,i(k),r} L_{S,k,i(k),r} P_{tx,i(k),r}}{\sigma^2 + \sum_{j \in J_k} L_{M,k,j,r} L_{S,k,j,r} P_{tx,j,r}} \tag{2}$$

where:

- $L_{M,k,i(k),r}$ and $L_{M,k,j,r}$ represent the propagation pathloss due to the distance and the antenna gain between the user k and its serving cell $i(k)$ and interfering cell $j \in J_k$, respectively;
- $L_{S,k,i(k),r}$ and $L_{S,k,j,r}$ represent the shadow fading pathlosses between the user k and its serving cell $i(k)$ and interfering cell $j \in J_k$, respectively;
- $P_{tx,i(k),r}$ is the transmitted power from serving cell $i(k)$ of user k;
- $P_{tx,j,r}$ is the transmitted power from the interfering cell $j \in J_k$;
- and σ is the power of the additive white Gaussian noise received by user k.

The second parameter of the COF is the interference limitation factor of the UE when it is associated to an ERC. The interference limitation factor permits the achievement of the DL-SINR target Γ_k of each user $k \in U$ while it is served by an ERC. Concretely, this parameter defines the highest interference that a user associated with an ERC (macrocell or picocell) can tolerate. Motivated by [10], the interference limitation factor can be defined as:

$$I_{k,r}^{max} = \frac{P_{rx,i(k),r}}{\Gamma_k} - \sigma^2 \tag{3}$$

where $P_{rx,i(k),r}$ is the DL-RSS measured by user k from the carrier signal sent by its serving ERC i in RB r.

The last parameter that builds the combined objective function is the cell load factor. In cellular networks, cell load can be measured by the level of resource usage at each cell/BS, which is given by:

$$\beta_i = \frac{\sum_{i \in B} \beta_{k,i}}{M} \tag{4}$$

- where M is the available resource units in BS i;
- $\beta_{k,i}$ is the amount of required resource of user k from BS i which is defined as:

$$\beta_{k,i} = \frac{d_{k,i}}{D \log_2(1 + y_k)} \tag{5}$$

- $d_{k,i}$ is the practical rate requirement of user k from BS i;
- and D is the available bandwidth.

Cell load is a positive value comprising between 0 and 1, $0 \leq \beta_i \leq 1$. A cell load value $\beta_i < 1$ means that cell radio resources can meet the user demand. When the cell load value is $\beta_i \approx 1$, there is a high probability of service outage and a congestion at several UEs. $\beta_i > 1$ will reveal that the cell is highly-loaded and the cell resources cannot meet the requirements of all UEs.

A. HANDOVER PROCEDURE IN HetNetsk

In cellular networks, handovers allow a UE to transfer their active connections from its serving cell to a target cell in connected mode, while maintaining QoS [17]. In conventional homogeneous networks, UEs typically use the same set of handover parameters (e.g. the hysteresis margin and time-to-trigger (TTT)) throughout the network. However, in Het-Nets, using the same set of handover parameters for all cells and/or for all UEs may degrade mobility performance [18]. In such cases, optimization of cell-specific handover parameters is required in HetNets. In this section, we describe major handover procedures for cellular networks and HetNets as defined in 3GPP.

1) CONVENTIONAL HANDOVER PROCEDURE

The conventional handover procedure in cellular networks has been discussed in [19] and is defined as:

$$P_{rx,p,k} > P_{rx,m,k} + HHM \tag{6}$$

In condition (6), a user k, which is associated with a serving MBS, is simply handed-over to a neighbouring PBS when its downlink RSRP $P_{rx,p,k}$ from PBS is stronger than $P_{rx,m,k}$ from MBS plus an offset denoted HHM. We define HHM as a positive-value parameter that is generally used to mitigate the handover ping-pong effect. Yet, HHM it is not sufficient to alleviate the ping-pong effect completely.

2) CELL RANGE EXPANSION (CRE) HANDOVER PROCEDURE

The CRE handover procedure has been proposed in [8]–[20], where related conditions are defined as:

$$P_{rx,p,k} + w_p > P_{rx,m,k} + HHM \tag{7}$$
$$P_{rx,m,k} > P_{rx,p,k} + w_p + HHM \tag{8}$$

Conditions (7) and (8) state the handover triggering procedure from macrocell to picocell and from picocell to

macrocell, respectively. Here, UEs can realize the expansion of picocell's region by adding a non-negative virtual offset w_p to the DL-RSS of the pilot signal $P_{rx,p,k}$ received from PBS. In fact, this will enable more UEs to be handed-over and served by an underloaded PBS. Nevertheless, w_p should be chosen properly in order to profit from the range expansion's efficiency, since an excessive value of w_p will considerably increase the resulting interference for users within the pico-cells' expanded range. Further, a low value of w_p will not have any impact on the global performance, such as load balancing or fairness.

3) COORDINATED RANGE EXPANSION HANDOVER PROCEDURE

Handover condition of a coordinated range expansion strat-egy for a user k to neighbouring PBS or MBS can be defined as:

$$P_{rx,m(p),k} + w_{m(p)} > P_{rx,p(m),k} + w_{m(p)} + HHM \qquad (9)$$

As stated above, in a conventional CRE procedure, only picocells are incited to expand their coverage. Conversely, via CCREMM in (9), both macrocell and picocell extend their DL coverage by allowing UEs to add a positive arti-ficial bias to the DL-RSS of the signal received from them (picocell and/or macrocell). The coordinated range expansion allows robustness of any mobility management technique for a medium to high user velocity environments. However, in a case of an aggressive CRE, the overall capacity of the network may deteriorate since aggressive range expansion will lead into overloading of some cells and/or excessive DL-ICI. Thus it is crucial to optimally set the value of $w_{m(p)}$ and to utilize a robust interference mitigation strategy to benefit from the power of range expansion. Problems related to load imbalance and ICI are addressed in the following sections.

III. COORDINATED CELL RANGE EXPANSION FOR MOBILITY MANAGEMENT (CCREMM) STRATEGY

As stated in our contributions, the main purpose of the work is to enhance the user association and mobility management efficiency in HetNets environments in which BSs differ in their coverage and transmit power, and when user mobility is considerable. It is to be noted that these characteristics cause various problems in HetNets, such as load imbalance, unfairness between UEs, and degradation of UE throughput. Consequently, we propose a partial solution to these issues by giving new analytical and optimal expressions for macrocell and picocell biases computation. To do so, we will exploit the efficiency of utility functions. Moreover, our CCREMM strategy utilizes a function that takes into account several parameters such as the QoS, ICI and LB, given in (1), (3), (4) respectively.

A. COMBINED OBJECTIVE FUNCTION DESIGN

In order to achieve the target enunciated above, we first design a COF $F_{m(p),k}$ that will enable us to build our utility functions to compute the macrocell and picocell artificial offsets. We have assumed in section II that $F_{m(p),k}$ is formed by three major factors, such as the QoS satisfaction, the inter-ference limitation and the cell load factors. The formulation of $F_{m(p),k}$ is given below:

$$F_{m(p),k} = w_{i(m,p)} \ln \left(\frac{N_{\beta_{i(m,p)}}}{N_{\Gamma_k} + N_{I_{k,r}^{\max}}} \right) \qquad (10)$$

where:
- $N_{\beta_{i(m,p)}}$ is the normalized load of the target macrocell or picocell defined in (4);
- $w_{i(m,p)}$ is the weight of the cost function which will be optimized to get the macrocell and picocell virtual REO;
- N_{Γ_k} is the normalized minimum UE QoS in terms of a target SINR, as defined in (1);
- $N_{I_k^{\max}}$ represents the normalized highest ICI that users of picocell's/macrocell's extended region can tolerate, it is defined in (3).

A multi-weighted linear objective function, in the form of (10), has been proposed by *D. Lee et al.* in [21]. The cost-function used in their work consists of a weighted summation of individual parameters related to the users speed and cell load, as well as the number of connected users. Thereafter, the result of the cost function is multiplied by an adjustment parameter, which is denoted by α, and it is incorporated into a standard RSS-based procedure as an additional HHM.

By using (10), we can design the utility functions that enable us to build equations for macrocell and picocell REO. Currently, utility functions are widely used in power control and interference mitigation algorithms. However, to the best of our knowledge, the concept of utility function has not been previously exploited in CRE-based UA and MM in HetNets.

B. MUE UTILITY FUNCTION AND OPTIMAL MACROCELL REO $\hat{w}_{i,m}$

In this section, we find the optimal REO value for each macrocell. Hence:
- the notation of the combined objective function in (10) becomes $F_{m,k}$;
- the cost function weight: $w_{i,m}$;
- and the macrocell load: $N_{\beta_{i(m)}}$.

Firstly, we use the standard definition of utility function for network BSs, which is composed of utility function $U_{m,k}$, representing the degree of satisfaction of UEs connected to MBS i, and a cost function C_k, representing the computa-tional cost incurred. The resulting total utility function $U_{Net,k}$ to be maximized for each macrocell is then expressed as follows:

$$U_{Net,k}\left(F_{m,k}\right) = U_{m,k}\left(F_{m,k}\right) - C_k\left(F_{m,k}\right) \qquad (11)$$

We define the utility function for each MUE $k \in U(m)$, so as to reflect its degree of satisfaction in terms of QoS as follows:

$$U_{m,k}\left(F_{m,k}\right) = \frac{1}{1 + \exp\left(-\alpha_{i,m}F_{m,k}\right)} \qquad (12)$$

Equation (12) is a Sigmoid function proposed in [22] as a utility function for a distributed power control scheme. In wireless cellular networks, it is used to compute the optimal value of each user's transmission power. In our work, we further use such a utility function at the macrocell in order to obtain its optimum bias for range expansion. The cost function is introduced to represent the increasing computational cost incurred by a more accurate offset value with minimized implementation errors. Yet, we cannot implement perfect biases in practice without inducing an increased computational burden. We define the same following cost function for each UE k, $\forall k \in U$ associated with MBS as:

$$C_k\left(F_{m,k}\right) = \delta_{i,m} F_{m,k} \tag{13}$$

Obviously, by maximizing the utility function $U_{m,k}$ in (12), the MUE is increasingly satisfied by the received QoS. Yet, the cost function C_k will be increased. The resulting total utility function $U_{Net,k}$ is obtained from (11) to (13) as:

$$U_{Net,k}\left(F_{m,k}\right) = \frac{1}{1 + \exp\left(-\alpha_{i,m} F_{m,k}\right)} - \delta_{i,m} F_{m,k} \tag{14}$$

In order to determine the optimal values of macrocell bias $\hat{w}_{i,m}$, we must compute the optimal cost function $\hat{F}_{m,k}$, which maximizes the total utility function $U_{Net,k}$ in (14). Therefore, we use the expression of the cost function in (13) and take the derivative of (11) with respect to the variable $F_{m,k}$ as follows:

$$U_k'\left(\hat{F}_{m,k}\right) - \delta = 0 \Leftrightarrow \hat{F}_{m,k} = U_k'^{-1} \tag{15}$$

We can express the COF in (10) as:

$$F_{m,k} = w_{i(m)} \ln O_{m,k} \tag{16}$$

with:

$$O_{m,k} = \frac{N_{\beta_{i(m,p)}}}{N_{\Gamma_k} + N_{I_{\max}^k}} \tag{17}$$

Consequently, from equations (10) and (15), we can express the optimal macrocell REO as:

$$\hat{w}_{i,m} = \frac{U_k'^{-1}}{\ln\left(O_{m,k}\right)} \tag{18}$$

By manipulating (14) and (18), the value of $\hat{w}_{i,m}$ can be deduced as:

$$\hat{w}_{i,m} = \frac{\left[\ln\left(\frac{\alpha_{i,m}}{\delta_{i,m}} - 1 - \sqrt{\left(\frac{\alpha_{i,m}}{\delta_{i,m}} - 1\right)^2 - 1}\right)\right]}{\alpha_{i,m} \ln\left(O_{m,k}\right)} \tag{19}$$

In (19), $\delta_{i,m}$ and $\alpha_{i,m}$ are respectively, the MUE pricing parameter and the steepness control parameter for the utility function in (12) that will be determined. Yet, we should verify that $\alpha_{i,m} \ln\left(O_{m,k}\right) \geq 0$. This condition is respected as long as $O_{m,k} \geq 1$ and $\delta_{m,k} \geq 0$. We assume that $\alpha_{i,m} > \theta_{i,m} \delta_{i,m}$, where:

- value of $\theta_{i,m}$ is fixed to:

$$\theta_{i,m} = \frac{\bar{w}_{i,m} \ln\left(F_{m,k}\right)}{2} \tag{20}$$

- and $\bar{w}_{i,m}$ is the maximum allowed bias for macrocell and its value will be revealed later.

C. PUE UTILITY FUNCTION AND OPTIMAL PICOCELL REO $\hat{w}_{i,p}$

Now that macrocell bias $\hat{w}_{i,m}$ has been defined, we determine the utility function below in order to compute the optimal REO $\hat{w}_{i,p}$ for each picocell. Since we try to find the optimal bias value in picocells:

- the notation of the COF in (10) becomes $F_{p,k}$;
- the cost function weight: $w_{i,p}$;
- and the macrocell load: $N_{\beta_{i(p)}}$

Similar to the MUE, for PUE $k \in U(p)$, we define the following utility function:

$$U_{p,k}\left(F_{p,k}\right) = F_{p,k} = w_{i,p} \ln\left(\frac{N_{\beta_{i(p)}}}{N_{\Gamma_k} + N_{I_{\max}^k}}\right) \tag{21}$$

The resulting total utility function $U_{Net,k}$ to be maximized at each picocell $i \in p$ is expressed as follows:

$$\begin{aligned} U_{Net,k}\left(F_{p,k}\right) &= F_{p,k}^x - \delta_{i,p} F_{p,k} \\ &= \left(w_{i,p} \ln\left(\frac{N_{\beta_{i(p)}}}{N_{\Gamma_k} + N_{I_{\max}^k}}\right)\right)^x - \delta_{i,p} F_{p,k} \end{aligned} \tag{22}$$

where $F_{p,k}^x$, defined in (22), is the utility function that represents the degree of user satisfaction and $\delta_{i,p} F_{p,k}$ is the cost function that represents the computational cost incurred, this is the same definition as in section III-B. The desirable value of the non-negative special parameter x is assumed to be $0 \leq x \leq \frac{1}{2}$ and $\delta_{i,p}$ is the pricing parameter δ of the PUE to be determined. The maximization of $U_{Net,k}$ yields an enhancement of the picocell UE throughput while accounting to the incurred computational price.

Thereafter, we take the first derivative of the total PUE utility function in (22) with respect to the variable $F_{p,k}$. Then we can obtain the best response $\hat{F}_{p,k}$ by setting the first derivative of (22) to zero. After some manipulations, the best response related to the total utility function $U_{Net,k}\left(F_{p,k}\right)$ can be obtained as follows:

$$\hat{F}_{p,k} = \frac{\delta_{i,p}^{1/x-1}}{x} \tag{23}$$

Finally, after some manipulations and using the same expression as in (18), we get the optimal picocell REO value $\hat{w}_{i,p}$ as:

$$\hat{w}_{i,p} = \frac{\delta_{i,p}^{1/x-1}}{x \ln\left(O_{p,k}\right)} \tag{24}$$

$O_{p,k}$ in (24) is defined as:

$$O_{p,k} = \frac{N_{\beta_{i(p)}}}{N_{\Gamma_k} + N_{I_{\max}^k}} \tag{25}$$

In (24), we should verify that the denominator $\ln\left(O_{p,k}\right) \geq 0$, this condition is fulfilled if $O_{p,k} \geq 1$.

D. MAXIMUM THROUGHPUT SCHEDULING (MTS)

The proposed CCREMM approach considers a throughput-based scheduling mechanism which is the maximum throughput scheduling (MTS) technique of [23] to schedule each user for each available RB. In MTS, Mutual Information Effective SNR Mapping (MIESM) is used to calculate an average channel quality indicator (CQI) value for all UE resources. This enables a rate increase while still guaranteeing an imposed Block Error Ratio (BLER) constraint. The scheduling is defined as a sum rate maximization problem formulated in (26). Then, at each RB r, a UE k is selected to be scheduled for RB r according to the following scheduling criterion:

$$\{r_1,\ldots,r_U\} = \arg\max_{\{r_1,\ldots,r_U\}} \sum_{k=1}^{U} T_k \qquad (26)$$

$$r_j^T . r_i = 0 \quad \forall i \neq j \qquad (27)$$

$$r_k(n) \in \{0,1\} \quad \forall n, k \qquad (28)$$

where T_k is the throughput of user k in bits/s and $r_k(n) \in \{0,1\}$ is a binary vector indicating which RBs are allocated to user k. Since the formulation above is a nonlinear binary integer problem, there exist no efficient solutions so far. Then the problem has been simplified to form a linearized model that approximates the nonlinear optimization problem.

E. SUMMARY OF THE CCREMM STRATEGY

In this section, we describe how the proposed CCREMM strategy is implemented in HetNets and also how it works concretely. In fact, both MBS and PBS collect information concerning the load, the average QoS of its associated UEs and their maximum tolerable interference. Each cell computes its optimum range expansion bias according to a combined objective function and utility functions formed by the aforementioned factors. After obtaining the optimal REO, a BS denoted by i decides which UE k to schedule on which RB r based on the MTS scheduler policy defined in (26). To provide a better overview, we present the CCREMM strategy flowchart in Figure 1. Furthermore, the algorithm summary is presented in Table I.

IV. SIMULATION RESULTS AND DISCUSSION
A. SIMULATION SCENARIO

In order to validate the model, we carry out computer simulations at the system level and give results in this section. The HetNets scenario used in the system-level simulations, as well as the UE and BS distribution, are based on the configuration 4b in [24]. Each macrocell area has two hotspots of a $40m$ radius, with each hotspot served by one pico BS. In the simulations, we consider seven hexagonal macrocell in which a macrocell consists of three sectors. One PBS is
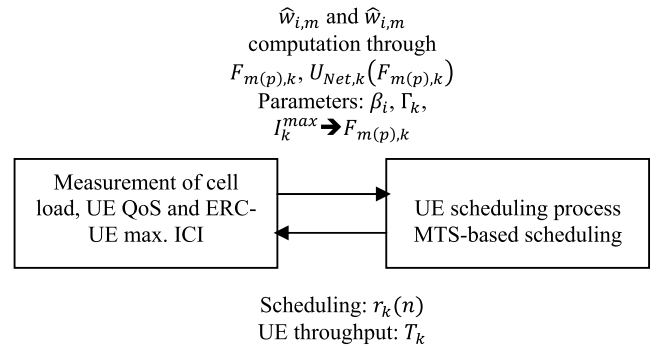

FIGURE 1. Flowchart of the proposed CCREMM strategy.

TABLE 1. Summary of the coordinated cell range expansion for mobility MANAGEMENT STRATEGY.

For each TTI
    For each RB r
    1-UE to RB scheduling using MTS policy
        For each BS i
            For each user k
    2-Each user $k \in U$ measures the DL-RSRP from its serving and neighboring BSs , estimates the pathloss and channel gains
    3-Then, $\beta_{i(m,p)}$ and $I_{k,r}^{max}$ can be deduced from 2.
    4-Each BS i acquires informations on load $\beta_{i(m,p)}$, QoS Γ_K and max. interference $I_{k,r}^{max}$
    5-Normalized $N_{\beta_{i(m,p)}}$, N_{Γ_K}, $N_{I_{k,r}^{max}}$ are deduced from 4. by using the general normalization formulation: $N_{x_i} = \frac{x_i - \min(x)}{\max(x) - \min(x)}$
    6-From 2. to 5., build the $O_{k,m(p)}$ in (10)
    7-If
        a-MBS: compute macrocell offset $\widehat{w}_{i,m}$ in (10) using equations (11) to (20)
        b-PBS: compute picocell offset $\widehat{w}_{i,p}$ in (10) using equations (21) to (24)
    8- Each BS computes the OF $F_{m(p),k}$ and evaluate the resulted cost incurred by applying a given virtual offset $\widehat{w}_{i,m}$, $\widehat{w}_{i,p}$
            End
        End
    End
End

RBs, resource blocks; UE, user equipment; TTI, transmission time interval; BS, base station; MBS, macro base station; PBS, pico base station; MTS, maximum throughput scheduler; OF, objective function; DL-RSRP, downlink received signal reference power; QoS, quality of service.

dropped randomly within each macrocell sector. Hence, in total, our HetNets is composed of 42 cells with 21 macrocell sector and 21 picocells.

There are two layers of users in the system with a total of 30 users in each macrocell:

- 1/3 of the users, i.e. 10 UEs, are randomly distributed throughout the coverage area of each macrocell;

• The remaining 2/3 of users are randomly and uniformly dropped within a radius of 40*m* of each PBS or picocell center.

All generated users have an omnidirectional antenna with 0*dBi* antenna gain. Further simulation parameters are summarized in Table 2. The cell layout is illustrated in Figure 2.

TABLE 2. Simulation parameters.

Parameters	Macrocell	Picocell
Carrier frequency	2 Ghz	
Bandwidth	10 Mhz	
Subframe duration	1 ms	
Traffic model	Full buffer (continuous traffic)	
Scheduling policies	Propodtional fair, Maximum throughput	
N	50 RBs	
	12 subcarriers per RB	
Transmission mode	Transmit diversity	
Thermal noise level	-174 dBm/Hz	
Initial UEs number	30 UEs per macrocell	
Lognormal shadowing	10 dB/8 dB – Fast fading	
Cell layout	Hexagonal grid of seven cells, three sectors per cell	Circular cell, one sector per cell
Transmit power	46 dBm	30 dBm
Pathloss model	128.1 + 37.6 log10 (R) R in km	140.7 + 37.6 log10 (R) R in km
UEs distribution radius	289 m	40m
Antenna gain	14 dBi	5 dbi
UE average speed	3 km/h	
Simulation time in TTIs	1000	
CCREMM strategy parameters	$\delta_{i,m}$ $= \{2,4,6,8,10\}$ $\alpha_{i,m} > \theta_{i,m}\delta_{i,m}$ $\theta_{i,m}$ $= \dfrac{\overline{w}_{i,m}\ln(F_{m,k})}{2}$ $\overline{w}_{i,m} = 10dB$	$\delta_{i,p} = \{2,4,6,8,10\}$ $0 \leq x \leq \frac{1}{2}$.
TTT	480ms	

RBs, resource blocks; UE, user equipment; TTI, transmission time interval; CCREMM, coordinated cell range expansion for mobility management; TTT, time to trigger.

B. CCREMM COMPUTATIONAL COMPLEXITY

The CCREMM strategy proposed in this paper requires a limited amount of measurement report exchange. In fact, the UE and its serving BS cooperate to build the neighboring cells list, and estimate the pathloss between it and its neighbouring cells. Moreover, the UE and its serving macrocell exchange measurement reports to update the list of neighboring cells. The UE receiver is then able to estimate the channel gains exploiting the pilot channels received from these cells and compute the received power from them.

Through simulations, the effectiveness of CCREMM will be shown. However, the coordinated process becomes increasingly complex when selecting a larger number of
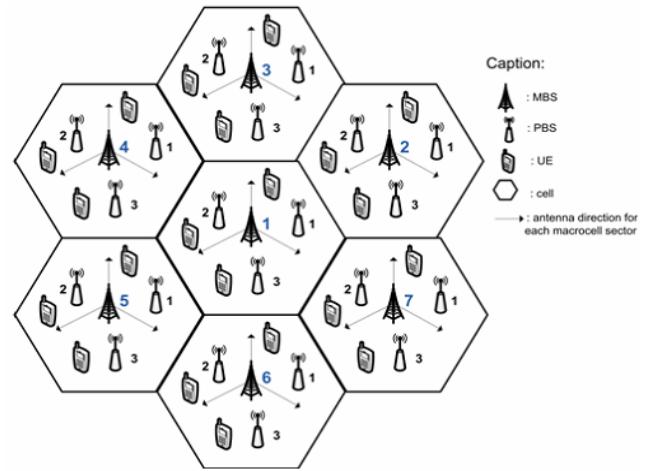

FIGURE 2. Illustration of a wrap-around hexagonal network of sectorized cells with the antenna orientations for each sector. This is the HetNets configuration used in the system level simulations. Recall that wihtin each MBS sector, one PBS is spreaded randomly and UEs are distributed randomly and uniformly within each MBS and PBS. Due to space limitation, we have only draw one UE per PBS but the real nUEs per BS is given in section IV-A.

control parameters $\delta_{i,m}$ and $\delta_{i,p}$. In fact, the number of possibilities resulted from a large set of $\delta_{i,m}$ and $\delta_{i,p}$ will increase the implementation complexity of the proposed CCREMM in a real-time network. Hence, to further limit the computational cost increase in the proposed utility functions, we select appropriately some of these parameters combination possibilities (i.e. $\delta_{i,m}$ and $\delta_{i,p}$) that minimizes the COF in (10) and compare their behaviour.

On an average computer, macrocell REO computation time for each value of $\delta_{i,m}$ is about 0.25*s*. On another side, picocell REO computation for each value of $\delta_{i,p}$ is about 0.084*s* if $nLPNs = 1$ per macrocell sector. For$nLPNs = 2$, running time of $\hat{w}_{i,p}$ is 0.085*s* and for $nLPNs = 4$, it is 0.086*s*. We observe first that the increase in the nLPNs doesn't necessarily enhance extraneously the computation time of the REO. Secondly, there is a considerable difference between running time of macrocell and picocell REO computation. This could be explained by the fact that the equation for $\hat{w}_{i,m}$ in (19) is heavier than that of $\hat{w}_{i,p}$ in (24). The equation (19) implies more parameter adjustment to be optimized than (24).

The total simulation time in a HetNet when applying the CCREMM strategy (presented in Figure 1 and Table 1) and including the measurement reports exchange is 4*mn* 3*s* for 10 *TTIs* having duration of 1*ms* each. The total simulation time in a HetNet without CCREMM is about4*mn* 19*s*. Hence we can deduce that our CCREMM mechanism could be implemented in a real-time network when considering a reasonable number of parameters to be optimized.

C. PERFORMANCE EVALUATION OF CCREMM FOR DIFFERENT VALUES OF $\delta_{i,m}$ AND $\delta_{i,P}$

We fist note that a robust and efficient mobility management approaches must not only enhance the performance of the network in terms of UE throughput and SINR but also the

performance in terms of handover. Consequently, handovers are simulated in this work. We use a standard $TTT = 480ms$ [17], [18] and we obtain results on UE throughput and SINR. However, due to space limitation, we omit results on handover failure and ping-pong probabilities in this paper but we will include them in another paper as a function of several TTT values.

The performance of our proposed CCREMM strategy depends on the tuning of parameters, mainly the control parameters $\delta_{i,m}$ and $\delta_{i,p}$. In order to get optimal macrocell and picocell bias $\hat{w}_{i,m}$ in (19) and $\hat{w}_{i,p}$ in (24), we have to adjust dynamically the non-negative pricing parameters $\delta_{i,m}$ and $\delta_{i,p}$ for macrocell and picocell, respectively. We recall that, for macrocell, $\alpha_{i,m} > \theta_{i,m}\delta_{i,m}$ and the non-negative control parameter $\theta_{i,m}$ is given in (20) (with $\bar{w}_{i,m}$ being the upper bound on the maximum allowed macrocell's bias, $\bar{w}_{i,m} = 10dB$).

Then, we present some results regarding the performance variation in terms of user throughput and the SINR cumulative distribution function (CDF) for the CCREMM strategy with MTS. To get these results, we apply different values of macrocell and picoll price parameters $\delta_{i,m}$ and $\delta_{i,p}$, such as $\{\delta_{i,m}, \delta_{i,p}\} = \{2, 4, 6, 8, 10\}$. Moreover, variation on our combined objective function $F_{m(p),k}$ in (10) is depicted for various $\delta_{i,m}$ and $\delta_{i,p}$ and the cost incurred by selecting a given parameter value is shown. However, finding best values in sets $\delta_{i,m}$ and $\delta_{i,p}$ quickly becomes complex if one assumes that they are matrixes having a large size of $m \times n$.

Thus, vector $\{\delta_{i,m}, \delta_{i,p}\}$ could involve extraneous parameters' combinations possibilities. For the vector given above, the number of testing is equivalent to $n[\delta_{i,m}, \delta_{i,p}] = 25$. Yet, testing and simulating all possibilities is time consuming and at the same time will enhance the complexity of the algorithm. As we have mentioned in section IV.B, we select appropriately some of parameters that minimize the COF in (10). In fact, results for $\{\delta_{i,m}, \delta_{i,p}\} = \{2, 2\}$; $\{\delta_{i,m}, \delta_{i,p}\} = \{4, 2\}$; $\{\delta_{i,m}, \delta_{i,p}\} = \{8, 8\}$ and $\{\delta_{i,m}, \delta_{i,p}\} = \{10, 6\}$ are depicted bellows. We assume that nLPNs = 1.

Figure 3 depicts the performance on UE throughput CDF for different values of $\delta_{i,m}$ and $\delta_{i,p}$. Here, performance is approximately 15% more significant for $\{\delta_{i,m}, \delta_{i,p}\} = \{2, 2\}$; $\{\delta_{i,m}, \delta_{i,p}\} = \{8, 8\}$ and $\{\delta_{i,m}, \delta_{i,p}\} = \{10, 6\}$ compared to $\{\delta_{i,m}, \delta_{i,p}\} = \{4, 2\}$ at some points. Generally speaking, however, all results from these combinations show acceptable user throughput which is due to the use of the MTS scheduler that permits the achievement of greater throughput than other standard schedulers. Indeed, MTS is a MIESM-based feedback strategy that has been proven to achieve close to optimal performance in terms of throughput while fulfilling an imposed constraint on a maximum allowed BLER [24].

In figure 4, performance variation in terms of user SINR CDF is shown for various values of $\delta_{i,m}$ and $\delta_{i,p}$ (that minimize the COF). We observe that almost the same SINR gain is obtained for $\{\delta_{i,m}, \delta_{i,p}\} = \{4, 2\}$ and $\{\delta_{i,m}, \delta_{i,p}\} = \{8, 8\}$, where user's QoS satisfaction in terms of target SINR is nearly 40% greater comparing to $\{\delta_{i,m}, \delta_{i,p}\} = \{2, 2\}$ and
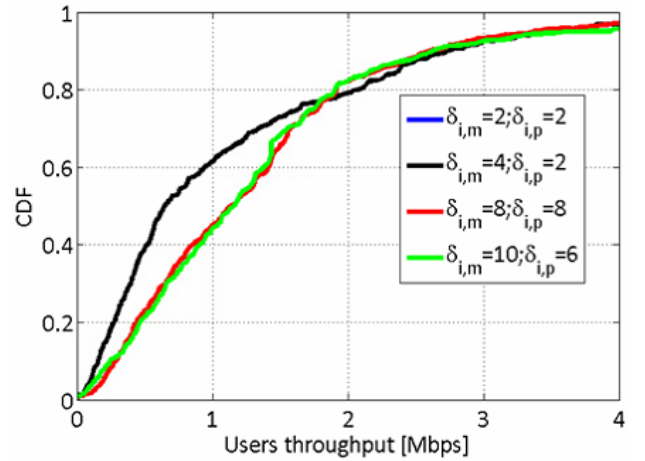

FIGURE 3. User throughput CDF in Mbits/s for different values of pricing parameters $\delta_{i,m}$ and $\delta_{i,p}$.
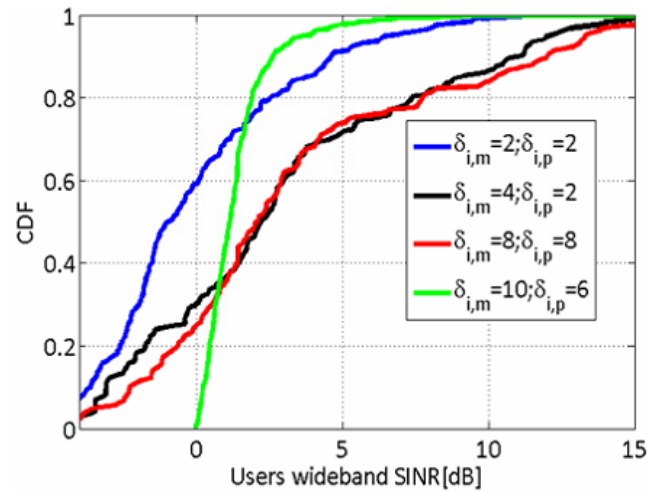

FIGURE 4. User wideband SINR in *dB* for different values of pricing parameters $\delta_{i,m}$ and $\delta_{i,p}$.

$\{\delta_{i,m}, \delta_{i,p}\} = \{10, 6\}$ which give less attractive performance for the actual metric. In figure 4, the achievement of the UE target SINR results from the integration of the interference cancelation criterion in the COF analyzed in (10) that partially mitigates the ICI at ERC-UE.

Figure 5 depicts the cost incurred by selecting specific combinations of $\delta_{i,m}$ and $\delta_{i,p}$. In fact, $\{\delta_{i,m}, \delta_{i,p}\} = \{2, 2\}$ results in the lowest cost while $\{\delta_{i,m}, \delta_{i,p}\} = \{8, 8\}$ and $\{\delta_{i,m}, \delta_{i,p}\} = \{10, 6\}$ induce the highest cost, as we can see in the figure. Another observation in Figure 5 is that the objective's price varies considerably when $\sum \delta$ increases. However, we require less fluctuation of the cost incurred by the objective function. In addition, we require the cheapest objective function's cost (i.e the minimum cost of the COF) since it could be more favorable for the CCREMM strategy.

As stated in section 3, CCREMM combined objective function aims to lower the resulted interference from CRE, enhance the network load balancing and satisfy user QoS
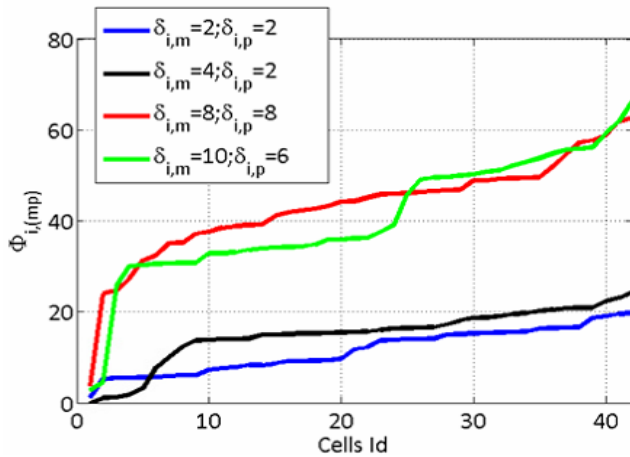
FIGURE 5. Cost fluctuation of the combined objective function $F_{m(p),k}$ in HetNets.

FIGURE 6. Users distribution in HetNets for static and dynamic UA approaches vs CCREMM $\{\delta_{i,m}, \delta_{i,p}\} = \{4, 2\}$.

in terms of target SINR. Consequently, we should select the set of $\delta_{i,m}$ and $\delta_{i,p}$ that gives the lowest cost but at the same time doesn't degrade either the user's throughput or the SINR. Yet, reaching all these objectives simultaneously is practically impossible, due to the trade-offs that exist between these performance metrics. Accordingly, we should define which one is the most important in order to achieve user satisfaction.

Judging from the information presented in Figures 3 to 5, and assuming that some trade-offs exist between the cited performance metrics, the best choice is $\{\delta_{i,m}, \delta_{i,p}\} = \{4, 2\}$, since it presents an interesting compromise between user throughput and SINR, as well as objective function's price.

D. PERFORMANCE EVALUATION OF CCREMM AGAINST SEVERAL CRE BENCHMARKS

Here, we consider various benchmarks used in literature in order to evaluate the performance of our CCREMM proposed scheme. We note that all the cited references below aim to achieve network load balancing by exploiting the strength of the CRE technique. As a first benchmark, we propose the fixed non-coordinated cell range expansion (FNCCRE-10), as used in [25], for a performance evaluation. In fact, FNCCRE-10 is the regular picocell range expansion technique that applies a fixed value of power bias to expand the picocell coverage area, which, in this case, is $w_{i,p} = 10 \, dB$.

The second benchmark is the technique proposed in [26] that we have called dynamic non-coordinated cell range expansion (DNCCRE) method. Those authors employ the concept of cell-load coupling. First, they assume that in HetNets, each cell's load depends on the load of other cells, in a nonlinear manner, due to the mutual coupling of interference observed by one another. Then, for a predefined offset vector, a statistical design of experiments (DOE) approach is applied in order to find optimal heterogeneous picocells offsets.

The last benchmark used in the performance comparison is the conventional CRE method, which is used as an evaluation method in [10], where $w_{i,p} = 6dB$. As in the first benchmark
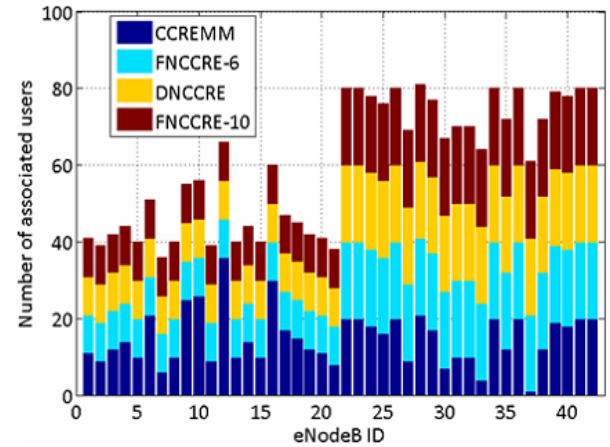
mentioned above, the picocells' range is expanded by adding a virtual offset to the received power.

Generally, in FNCCRE-10 and FNCCRE-6, values are obtained through a greedy search technique and are homogeneous for all picocells. However, applying such identical picocells biases does not always ensure performance efficiency in terms of load balancing or throughput, since excessive bias will overload picocells and insufficient bias will not solve the load unbalancing and unfairness problems in HetNets. In both cases, the network global performance is not distinctly improved through the use of a fixed uncoordinated range expansion technique.

The difference between these three benchmarks is that the first and third techniques are homogeneous and the second one is heterogeneous. However, they are all uncoordinated strategies (i.e there is no information exchange among cells). For the remaining comparisons in the paper, macrocell and picocell non-negative parameters are set to $\{\delta_{i,m}, \delta_{i,p}\} = \{4, 2\}$, respectively, and nLPNs = 1. Furthermore, the MTS scheduler is used jointly with CCREMM, and a PF scheduler is used for FNCCRE-6, FNCCRE-10 and DNCCRE. Recall that $\delta_{i,m}$ and $\delta_{i,p}$ are the most important parameters used in tuning our CCREMM strategy to compute the optimum REO $\hat{w}_{i,m}$ and $\hat{w}_{i,p}$ in order to maximize profit from them.

Figure 6 depicts the user's distribution among cells in HetNets for various methods, including our proposed CCREMM. For FNCCRE-10, FNCCRE-6 and DNCCRE, picocells serve too many users. The availability of resources in small cells 22 to 42 is maintained with our scheme, which is not the case for the other schemes. Since the small cells have limited resources, resources would not be sufficient for a large number of users offloaded to picocells. Consequently, offloaded users resulted from FNCCRE-10, FNCCRE-6 and DNCCRE may not attain their QoS requirements. At the same time, our proposed CCREMM allows for the offloading of users to light loaded picocells while keeping a number of users associated with macrocells, which guarantees users satisfaction in terms of QoS. For CCREMM, the number of offloaded users is
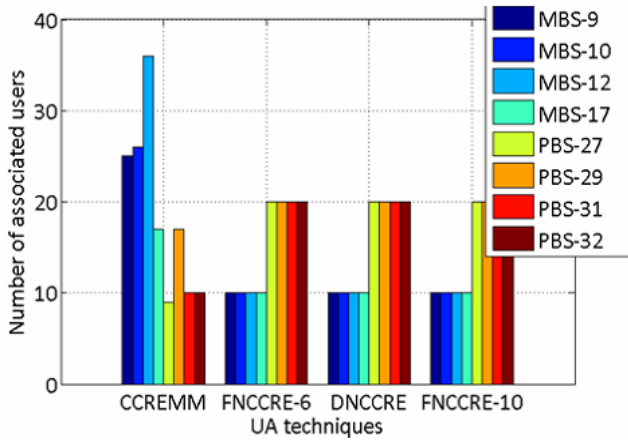
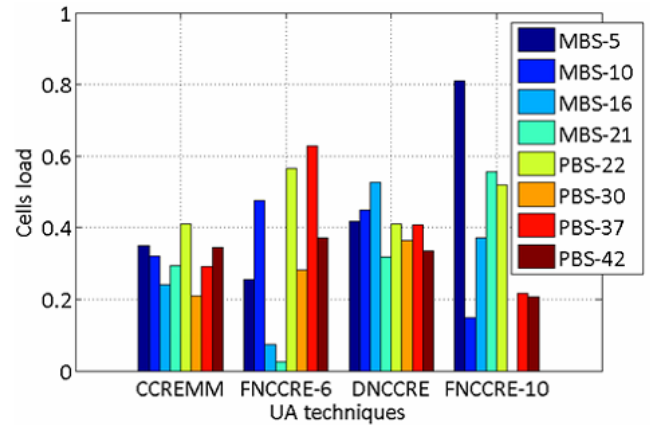**FIGURE 7.** Users distribution in Hetnets considering selected BSs, for clarification of Figure 6.

FIGURE 9. Cell load in Hetnets considering selected BSs, for clarification of Figure 8.
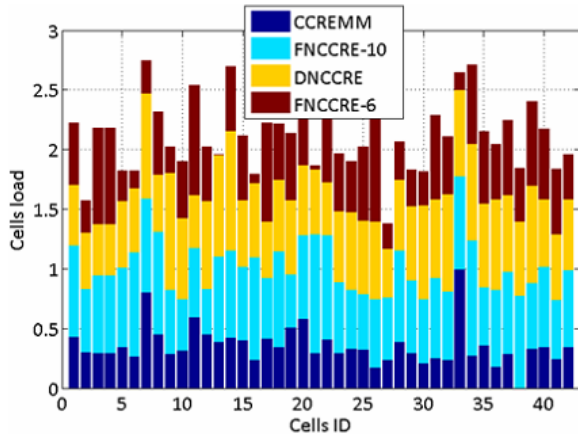

FIGURE 8. Normalized cell load in HetNets for static and dynamic UA approaches vs CCREMM $\{\delta_{i,m}, \delta_{i,p}\} = \{4, 2\}$.
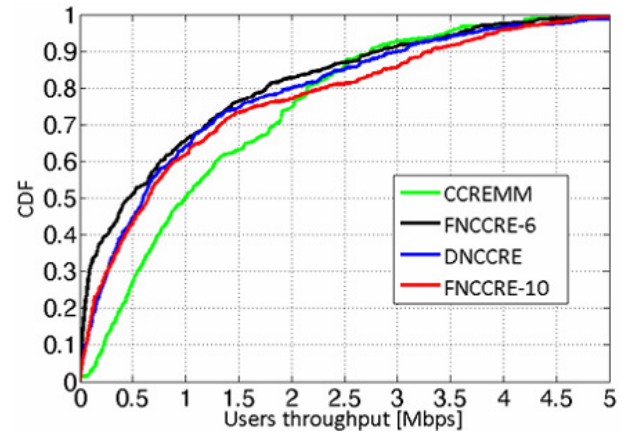

FIGURE 10. User throughput in Mbits/s, benchmarks vs CCREMM with $\{\delta_{i,m}, \delta_{i,p}\} = \{4, 2\}$.

not extraneous. To clarify the observation above, we focus on some examples of user's distribution among several BSs in Figure 6. This illustration is shown in Figure 7. At macro BSs 9, 10, 12 and 17, the number of users (nUEs) for the proposed CCREMM may pique our interest since these macro BSs serve a significant nUEs, compared to the remaining BSs and they serve a large nUEs compared to FNCCRE-6, DNCCRE and FNCCRE-10. This is due to the fact that the number of available resources is widely large in macro BSs 9, 10, 12 and 17, and maintaining connexion with them enables users to enhance their throughput.

In contrast, pico BSs 27, 29, 31, and 32 show lower offloading for CCREMM compared to FNCCRE-6, DNCCRE and FNCCRE-10. Actually, by optimal biasing, there is a lower risk of PBS overload. Our strategy ensures simultaneously cell load balancing and favorable user throughput.

In Figure 8, cell load resulting from several techniques, such as FNCCRE-6, FNCCRE-10, DNCCRE and CCREMM, is illustrated. We observe more cell load fairness for the proposed CCREMM compared to benchmarks. To illustrate, several BSs will be selected to examine

their resulting performance. This illustration is shown in Figure 9. For macro BSs 1 to 15, more load balancing is seen for CCREMM and DNCCRE compared to static UA techniques. Next, we observe that macro BSs 16 and 21 are the least loaded at FNCCRE-6, and they are the most loaded at FNCCRE-10, compared to the other UA techniques. Finally, for pico BSs 22 to 42, the mean cell load is almost equal for all picos when applying CCREMM; this is not observed in the three benchmarks. These behaviours once again demonstrate the efficiency of our proposed strategy in terms of load balancing. For the other methods, a worse result is obtained for static UA schemes. As stated earlier, selecting fixed association's techniques is sometimes risky since excessive bias will overload picocells and insufficient bias will not solve the load unbalancing and unfairness problems. Consequently, power offsets should be set dynamically, depending on the characteristics of each cell.

Figure 10 highlights results regarding user throughput CDF. A performance of about 30% is obtained while jointly using CCREMM and MTS scheduler compared to FNCCRE-6, FNCCRE-10 and DNCCRE methods with a
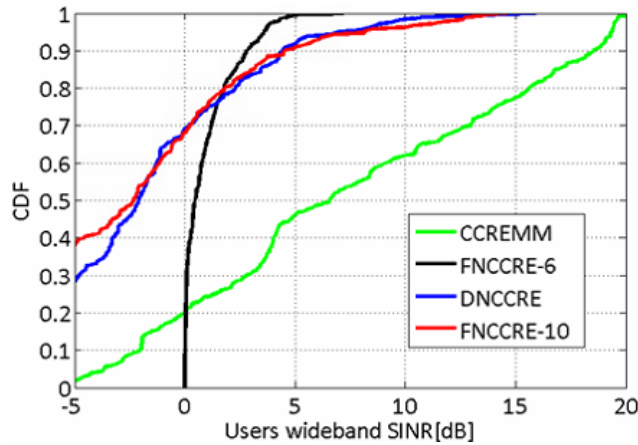
FIGURE 11. User wideband SINR in *dB* comparing benchmarks UA techniques vs CCREMM with $\{\delta_{i,m}, \delta_{i,p}\} = \{4, 2\}$.

FIGURE 12. Mean cell throughput in *Mbits/s*, benchmarks vs CCREMM with $\{\delta_{i,m}, \delta_{i,p}\} = \{4, 2\}$ and $nLPNs = \{1, 2, 4\}$.

FIGURE 13. Cell edge-user throughput in *Mbits/s*, benchmarks vs CCREMM with $\{\delta_{i,m}, \delta_{i,p}\} = \{4, 2\}$ and $nLPNs = \{1, 2, 4\}$.

conventional PF scheduler. The reason for such a result is that the proposed CCREMM aims both to satisfy the network in terms of rate and improve cell-edge users' throughput, which is reflected by the figure above. However, at some points, we can see that FNCCRE-10 outperforms CCREMM by 10% and the performance of CCREMM equals that of FNCCRE-6 and DNCCRE, i.e CCREMM becomes less efficient. We can interpret this in light of the fact that users associated with an expanded region picocell are sensitive to ICI since they are not connected to a BS that provides the strongest RSS. Though the proposed method permits mitigation of ICI by applying an upper bound I_k^{max} on the maximum tolerable ICI in the expanded cell's region, an extensive analysis should be performed to enhance its efficiency.

In Figure 11, a CDF of user SINR is presented, and there we notice a performance gain of around 95% for the proposed CCREMM versus other methods. We can deduce from this observation that a majority of users, if not all users, reach their target SINR, i.e their QoS satisfaction. This fact results from the utilization of the combined objective function $F_{m(p),k}$ that takes users' QoS requirements into account in order to design macrocell and picocell utility functions. Taken together, this information permits us to obtain optimum values of $\hat{w}_{i,m}$ and $\hat{w}_{i,p}$.

In the last four results, we perform simulations for the four techniques mentioned earlier and compare their performance in terms of user and cell throughput and fairness. We vary the number of picocells dropped in each macrocell area to $nLPNs = \{1, 2, 4\}$, which is a configuration used in [24]. In Figure 12, the average cell throughput is illustrated. An average cell throughput is the aggregate of the individual user's data rate in a cell. For each comparative method (FNCCRE-10, FNCCRE-6 and DNCCRE), performance is approximatively equal when $nLPNs = \{1, 2, 4\}$.

However, the obtained throughput in the proposed CCREMM outperforms those with benchmarks by almost 25% for all assumed nLPNs.

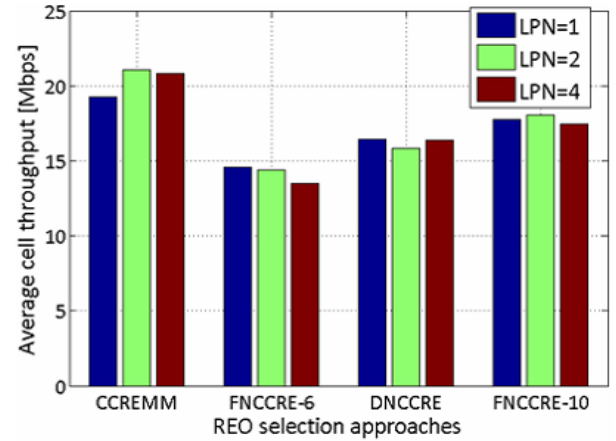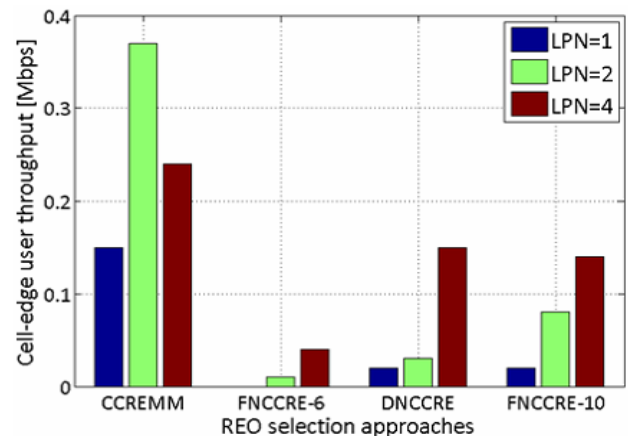A worse result is obtained for FNCCRE-6, and almost the same result is obtained for FNCCRE-10 and DNCCRE.

In fact, the CCREMM with MTS offers the highest number of bits to a large number of users, and this is illustrated by the performance of the cell's throughput in Figure 12.

Figure 13 depicts the performance in terms of edge user throughput for the four aforementioned techniques. Proposed CCREMM, which is adopted to compute optimum $\hat{w}_{i,m}$ and $\hat{w}_{i,p}$ widely outperforms the other association strategies for all assumed values of nLPNs. The Cell edge user's throughput gain is about 90% for the CCREMM, compared to others when $nLPNs = 1$. When $nLPNs = 2$ gains increase and when $nLPNs = 4$, the gain is about 35% more than DNCCRE and FNCCRE-6 and 85% more than FNCCRE-10. This observation means that at a lower picocell bias, the number of users offloading to picocells is low and large nUEs are handed over to macrocells, leading to macrocell overload and a low throughput for large nUEs. However, when bias is increased, user throughput is also enhanced, as more users are served by picocells.

Average UE throughput is depicted in Figure 14. This figure shows that the performance of FNCCRE-10, FNCCRE-6 and DNCCRE for $nLPNs = 1$ and $nLPNs = 2$ are
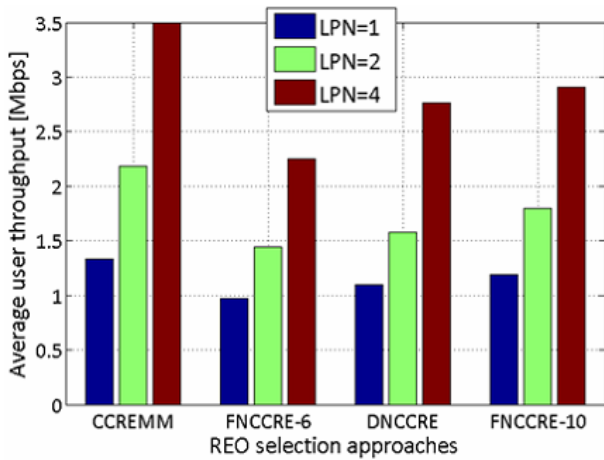
FIGURE 14. Mean user throughput in *Mbits/s*, benchmarks vs CCREMM with $\{\delta_{i,m}, \delta_{i,p}\} = \{4, 2\}$ and *nLPNs* = $\{1, 2, 4\}$.
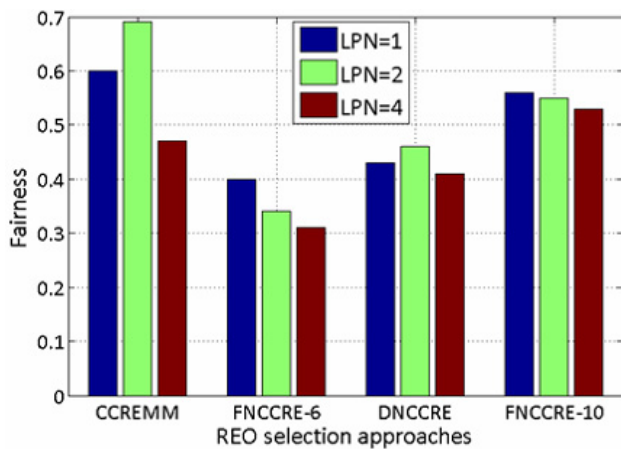

FIGURE 15. Resource allocation fairness, benchmarks vs CCREMM with $\{\delta_{i,m}, \delta_{i,p}\} = \{4, 2\}$ and *nLPNs* = $\{1, 2, 4\}$.

approximatively equal, although there is a slight improvement of between 15 and 20% for the CCREMM. In fact, an aggressive range expansion will not improve user throughput since an excessive bias will allow excessive user offloading to picocells, which in turn will decrease their satisfaction in terms of QoS. On the other hand, the CCREMM outperforms the other methods because it allows for the acquisition of dynamic optimum biases on macrocells and picocells through the exploitation of various parameters in a combined objective function. As a result, rate and user throughput are enhanced.

In Figure 15, user fairness performance in terms of resource allocation is illustrated for all comparative techniques by using the same formulation as in [27]. When compared to FNCCRE-6 and DNCCRE, the CCREMM shows higher performance mainly when $nLPNs = 1$ and $nLPNs = 2$. When compared to FNCCRE-10, a good result is still maintained when $nLPNs = 1$. An enhancement of between 5 and 20% is observed when $nLPNs = 2$. However, when $nLPNs = 4$, fairness in FNCCRE-10 surpasses that of the CCREMM. This difference can be explained by the

fact that when enhancing nLPNs in the network, logically, the number of users is enhanced greatly. Further, the CCREMM is a dynamic strategy which can lead to an excessive CRE at some point. In such a scenario, excessive number of UEs is offloaded to picocells; thus, the overloading of some picocells with poor resources is unavoidable. At the same time, users served by macrocells benefit from the availability of greater resources.

Finally, these effects create unfairness among picocell and macrocell users.

V. CONCLUSION

In this paper, we have proposed a CCREMM-based strategy for user association and mobility management in HetNets. It enables network load balancing, user fairness, users' QoS satisfaction, and interference limitation in such a network configuration. The proposed analytical strategy is based on new utility functions that have apparently not yet been exploited for a CCREMM in HetNets. These utility functions allow for the computation of values so as to enhance the cited-HetNets performance criterion. Hence, we have illustrated via system-level simulations that the suggested CCREMM strategy associated with the MTS scheduling can improve the LTE HetNets user and network throughput, and it can also enhance the users' wideband SINRs. Performance figures are shown to surpass those achieved by dynamic and fixed uncoordinated range expansion techniques. Finally, the proposed method surely enhances performance in terms of handover, with more extensive simulations.

REFERENCES

[1] A. Damnjanovic *et al.*, "A survey on 3GPP heterogeneous networks," *IEEE Wireless Commun.*, vol. 18, no. 3, pp. 10–21, Jun. 2011.

[2] H. S. Dhillon, R. K. Ganti, F. Baccelli, and J. G. Andrews, "Modeling and analysis of K-tier downlink heterogeneous cellular networks," *IEEE J. Sel. Areas Commun.*, vol. 30, no. 3, pp. 550–560, Apr. 2012.

[3] T. Q. S. Quek, G. de la Roche, I. Güvenç, and M. Kountouris, *Small Cell Networks: Deployment, PHY Techniques, and Resource Allocation*. Cambridge, U.K.: Cambridge Univ. Press, May 2013.

[4] J. G. Andrews, H. Claussen, M. Dohler, S. Rangan, and M. C. Reed, "Femtocells: Past, present, and future," *IEEE J. Sel. Areas Commun.*, vol. 30, no. 3, pp. 497–508, Apr. 2012.

[5] A. B. Saleh, Ö. Bulakci, S. Redana, B. Raaf, and J. Hämäläinen, "Enhancing LTE-Advanced relay deployments via biasing in cell selection and handover decision," in *Proc. IEEE Int. Symp. Pers. Indoor Mobile Radio Commun. (PIMRC)*, Istanbul, Turkey, Sep. 2010, pp. 2277–2281.

[6] Y. Bejerano and S.-J. Han, "Cell breathing techniques for load balancing in wireless LANs," *IEEE Trans. Mobile Comput.*, vol. 8, no. 6, pp. 735–749, Jun. 2009.

[7] *Mobility Enhancements in Heterogeneous Networks*. document 3GPP TR 36.839 V11.0.0, 3GPP, Sep. 2012.

[8] D. Xenakis, L. Merakos, N. Passas, and C. Verikoukis, "Mobility management for femtocells in LTE-advanced: Key aspects and survey of handover decision algorithms," *IEEE Commun. Surveys Tuts.*, vol. 16, no. 1, pp. 64–91, 1st Quart., 2014.

[9] M. Simsek, M. Bennis, and I. Guvenc, "Mobility management in HetNets: A learning-based perspective," *EURASIP J. Wireless Commun. Net.*, Feb. 2015, pp. 1–13.

[10] D. Lopez-Perez, X. Chu, and I. Guvenc, "On the expanded region of picocells in heterogeneous networks," *IEEE J. Sel. Topics Signal Process.*, vol. 6, no. 3, pp. 281–294, Jun. 2012.

[11] R. Madan, J. Borran, A. Sampath, N. Bhushan, A. Khandekar, and T. Ji, "Cell association and interference coordination in heterogeneous LTE-A cellular networks," *IEEE J. Sel. Areas Commun.*, vol. 28, no. 9, pp. 1479–1489, Dec. 2010.

[12] S. Singh and J. G. Andrews, "Joint resource partitioning and offloading in heterogeneous cellular networks," *IEEE Trans. Wireless Commun.*, vol. 13, no. 2, pp. 888–901, Feb. 2014.

[13] Q. Ye, B. Rong, Y. Chen, M. Al-Shalash, C. Caramanis, and J. G. Andrews, "User association for load balancing in heterogeneous cellular networks," *IEEE Trans. Wireless Commun.*, vol. 12, no. 6, pp. 2706–2716, Jun. 2013.

[14] K. Okino, T. Nakayama, C. Yamazaki, H. Sato, and Y. Kusano, "Pico cell range expansion with interference mitigation toward LTE-advanced heterogeneous networks," in *Proc. IEEE Intern. Conf. Commun. (ICC)*, Kyoto, Japan, Jun. 2011, pp. 1–5.

[15] T. Kudo and T. Ohtsuki, "Cell range expansion using distributed Q-learning in heterogeneous networks," *EURASIP J. Wireless Commun. Net.*, vol. 61, pp. 1–10, Mar. 2013.

[16] J. C. Ikuno, M. Wrulich, and M. Rupp, "System level simulation of LTE networks," in *Proc. IEEE Veh. Technol. Conf. (VTC)*, Tapei, Taiwan, May 2010, pp. 1–5.

[17] *Handover Procedures*, document 3GPP TS 23.009 V.11.0.0, 3GPP, Sep. 2011.

[18] D. Lopez-Perez, I. Guvenc, and X. Chu, "Mobility management challenges in 3GPP heterogeneous networks," *IEEE Commun. Mag.*, vol. 50, no. 12, pp. 70–78, Dec. 2012.

[19] H. Zhang, W. Ma, W. Li, W. Zheng, X. Wen, and C. Jiang, "Signalling cost evaluation of handover management schemes in LTE-advanced femtocell," in *Proc. IEEE Veh. Technol. Conf. (VTC)*, Budapest, Hungary, May 2011, pp. 1–5.

[20] *Mobility Enhancements in Heterogeneous Networks*, document TR 36.839V11.0.0, 3GPP, Sep. 2012.

[21] D.-W. Lee, G.-T. Gil, and D.-H. Kim, "A cost-based adaptive handover hysteresis scheme to minimize the handover failure rate in 3GPP LTE system," *EURASIP J. Wireless Commun. Netw.*, vol. 6, pp. 1–7, Feb. 2010.

[22] M. Xiao, N. B. Shroff, and E. K. P. Chong, "A utility-based power-control scheme in wireless cellular systems," *IEEE/ACM Trans. Netw.*, vol. 11, no. 2, pp. 210–221, Apr. 2003.

[23] S. Schwarz, C. Mehlführer, and M. Rupp, "Low complexity approximate maximum throughput scheduling for LTE," in *Proc. IEEE Asilomar Conf. Signal, Syst., Comput.*, Pacific Grove, CA, USA, Nov. 2010, pp. 1563–1569.

[24] *Further Advancements for E-UTRA Physical Layer Aspects, V.9.0.0*, 3GPP TR 36.814, 3GPP-TSG R1, Mar. 2010.

[25] J. G. Andrews, S. Singh, Q. Ye, X. Lin and H. S. Dhillon, "An overview of load balancing in hetnets: Old myths and open problems," *IEEE Wireless Commun.*, vol. 21, no. 2, pp. 18–25, Apr. 2014.

[26] I. Siomina and D. Yuan, "Load balancing in heterogeneous LTE: Range optimization via cell offset and load-coupling characterization," in *Proc. IEEE Int. Conf. Commun. (ICC)*, Ottawa, Canada, Jun. 2012, pp. 1357–1361.

[27] E. Rakotomanana and F. Gagnon, "Fair load balancing in heterogeneous cellular networks," in *Proc. IEEE Int. Conf. Ubiquitous Wireless Broadband (ICUWB)*, Montréal, QC, Canada. Oct. 2015, pp. 1–5.

[28] H. Zhang, C. Jiang, J. Cheng, and V. C. M. Leung, "Cooperative interference mitigation and handover management for heterogeneous cloud small cell networks," *IEEE Wireless Commun.*, vol. 22, no. 3, pp. 92–99, Jun. 2015.

EDENALISOA RAKOTOMANANA (S'13) received the M.Sc. degree in electrical engineering from the Institut National de la Recherche Scientifique, Montréal, Canada, in 2010. She is currently pursuing the Ph.D. degree with the LACIME Laboratory, École de Technologie Supérieure, Montréal, Canada. Her Ph.D. is part of the NSERC-Ultra Electronics Industrial Chair in Wireless Emergency and Tactical Communication. Her research interest covers mobility management and resource allocation in heterogeneous cellular networks.

FRANÇOIS GAGNON (SM'99) received the B.Eng. and Ph.D. degrees in electrical engineering from École Polytechnique de Montréal, Montréal, QC, Canada. He was the Chair of the Department of Electrical Engineering, École de Technologie Supérieure (ÉTS), Montréal, QC, Canada, from 1999 to 2001. He has been a Professor with the Department of Electrical Engineering, ÉTS, since 1991, and is currently the holder of the NSERC Ultra Electronics Chair, Wireless Emergency and Tactical Communication. His research interests include wireless high-speed communications, modulation, coding, high-speed DSP implementations, and military point-to-point communications. He has been involved in the creation of the new generation of high-capacity line-of-sight military radios offered by the Canadian Marconi Corporation, which is now ultraelectronics tactical communication systems.

● ● ●